Università degli Studi Mediterranea di Reggio Calabria
Archivio Istituzionale dei prodotti della ricerca

Seismic soil classification of Italy based on surface geology and shear-wave velocity measurements

This is the peer reviewd version of the followng article:

Original
Seismic soil classification of Italy based on surface geology and shear-wave velocity measurements / Forte, G., Chioccarelli, E., De Falco, M., Cito, P., Santo, A., Iervolino, I.. - In: SOIL DYNAMICS AND EARTHQUAKE ENGINEERING. - ISSN 0267-7261. - 122:(2019), pp. 79-93. [10.1016/j.soildyn.2019.04.002]

Availability:
This version is available at: https://hdl.handle.net/20.500.12318/60348 since: 2020-12-28T11:29:57Z

Published
DOI: http://doi.org/10.1016/j.soildyn.2019.04.002
The final published version is available online at:https://www.sciencedirect.

Terms of use:
The terms and conditions for the reuse of this version of the manuscript are specified in the publishing policy. For all terms of use and more information see the publisher's website

Publisher copyright

This item was downloaded from IRIS Università Mediterranea di Reggio Calabria (https://iris.unirc.it/) When citing, please refer to the published version.

(Article begins on next page)

24 June 2026

Seismic soil classification of Italy based on surface geology and shear-wave velocity measurements

Giovanni Forte[1], Eugenio Chioccarelli[2], Melania De Falco[1], Pasquale Cito[3], Antonio Santo[1], Iunio Iervolino[3]

[1]*Dipartimento d'Ingegneria Civile, Edile e Ambientale, Università degli Studi di Napoli Federico II, via Claudio 21, 80125 Naples, Italy.*
giovanni.forte@unina.it; melania.defalco@unina.it; santo@unina.it
[2]*Università Telematica Pegaso, piazza Trieste e Trento 48, 80132 Naples, Italy.*
eugenio.chioccarelli@unipegaso.it
[3] *Dipartimento di Strutture per l'Ingegneria e l'Architettura, Università degli Studi di Napoli Federico II, via Claudio 21, 80125 Naples, Italy.*
pasquale.cito@unina.it; iunio.iervolino@unina.it

Abstract

During an earthquake the seismic wave amplification related to local site conditions can have a significant impact on the ground motion characteristics. In order to account for these local effects some proxies for the soil characteristics exist; e.g., the average shear-wave velocity of the upper 30 meters $\left(V_{S,30}\right)$, or the equivalent shear-wave velocity from the ground to the depth of the seismic bedrock when this is less than 30 meters $\left(V_{S,eq}\right)$.

The aim of this paper is to provide maps of seismic shallow soil classification for Italy accounting for two sources of information: site-specific measurements and large-scale geological maps. The soil maps are obtained via a four-step procedure: (1) a database of available site-specific investigations is built, covering (unevenly) the whole national territory; (2) twenty geo-lithological complexes are identified from the available geological maps; (3) the investigations are grouped as a function of the geo-lithological complex and the distribution of measured $V_{S,30}$ and $V_{S,eq}$ are estimated; (4) medians and standard deviations of such distributions are assumed to be representative of the corresponding complexes. The statistics of investigations are used to derive the large-scale soil maps. To make the results of the study available, a stand-alone software has been developed. Despite not being adequate substitutes of site-specific studies such as microzonation and local site response analyses, the provided results can be useful for large-scale seismic risk studies.

Keywords: probabilistic seismic hazard assessment, regional seismic risk, site classification, soil classes, seismic soil response

1. Introduction

Seismic fault ruptures generate waves that propagate in all directions through the rigid bedrock for kilometres. Before reaching the ground surface, seismic waves go through the shallower materials covering the bedrock. It is known that this last part of propagation may have significant effects on a number of ground motion parameters (e.g., peak ground acceleration, spectral ordinates, etc.). Indeed, the so-called local site effects are deeply discussed in the literature (e.g., [1]) and must be taken into account for the estimation of seismic effects on engineering structures. This is pointed out by the landmark papers of Dobry and Vucetic [2] and Seed et al. [3] and is systematically confirmed by the distribution of observed damages after significant earthquakes (e.g., [4–6]). In the hypothesis of a uniform layer of isotropic, linear elastic soil overlying rigid bedrock, the soil amplification of a harmonic horizontal motion of the bedrock is a function of (i) the thickness of the soil layer and (ii) the propagation velocity of shear-waves. In real cases, seismic waves propagation is more complicated and *site response analysis* is required to characterize the peculiar soil dynamics (e.g., [7,8]). However, for the cases in which such analyses cannot be performed, a simplified parameter to account for the site response, the average shear-wave velocity of the upper 30 m, $V_{S,30}$, was proposed at the end of the last century ([9,10]). $V_{S,30}$ is defined as per Equation (1) where N is the number of homogeneous soil layers up to thirty meters depth whereas h_i and $V_{S,i}$ are the thickness and the shear-wave velocity (V_S) in the soil layer i, respectively.

$$V_{S,30} = \frac{30}{\sum_{i=1}^{N} \frac{h_i}{V_{S,i}}} \quad (1)$$

The depth of 30 m was conventionally assumed as relevant (it is, typically, a depth that can be attained in one working day of boring). The value of $V_{S,30}$ has the advantage of being easily obtainable, at relatively low cost, by performing in-hole (*Down-Hole* or DH, *Cross-Hole* or CH), or surface (SASW, MASW, Microtremors) geophysical tests (e.g., [11]). Furthermore, several scientific studies (e.g. [12–14]) provided strategies to infer $V_{S,30}$ values from the most common in-field tests, such as standard penetration test (SPT) or cone penetration test (CPT).

Today, $V_{S,30}$ is the main single-value parameter that summarizes seismic soil behaviour. The majority of the ground motion prediction equations (GMPEs) refer to $V_{S,30}$ either by (i) directly considering the $V_{S,30}$ value in the functional form (e.g., [15–18]); (ii) categorizing the soil behaviour (e.g., stiff or soft soil) depending on $V_{S,30}$ intervals and defining dummy variables associated to each soil category (e.g., [19,20]) or (iii) allowing both of these strategies (e.g., [21,22]). $V_{S,30}$ is also adopted by several seismic codes to identify the appropriate site-dependent design spectrum for structures; some examples are NEHRP Provisions [23] and the Eurocode 8, or EC8 [24].

On the other hand, several authors highlighted that knowledge of $V_{S,30}$ may not be enough to properly quantify the variation of seismic motion from bedrock to ground surface (see for example [25–28]). Indeed, it is known that the overall tendency of V_S is to increase with depth; nevertheless, actual soil profiles may exhibit a shallow velocity inversion, due to the soil depositional variability along the profiles, which is reflected in peculiar characteristics of the seismic signal propagated through them. This case, in fact, cannot be detected if only the $V_{S,30}$ parameter is considered. Similarly, $V_{S,30}$ is not able to account for non-linear soil behaviour, for the actual depth of seismic bedrock, for deep soft deposits lying on much stiffer rock, for velocity profiles that do not exhibit a strong impedance contrast in the first meters or in basin-type geological settings. Thus, in the last years, scientific efforts

have been made to develop and update classification criteria based on $V_{S,30}$ together with other relevant parameters, such as the bedrock depth (e.g., [29]), or site period/frequency (e.g., [30]). In accordance with this trend, the recent Italian building code, or ItBC2018 [31], tries to overcome some of the $V_{S,30}$ limitations (those related to bedrock depth), by referring to the so-called $V_{S,eq}$, which derives from a slight modification of the $V_{S,30}$ parameter. This is defined in Equation (2), in which H is the depth of the bedrock if it is less than 30 meters. When the bedrock is deeper, H is equal to 30 (and $V_{S,eq}$ degenerates into $V_{S,30}$).

$$V_{S,\mathrm{eq}} = \frac{H}{\sum_{i=1}^{N} \frac{h_i}{V_{S,i}}} \tag{2}$$

It should be noted that, although $V_{S,30}$ or $V_{S,eq}$ can be useful for a preliminary soil site classification, they cannot be considered as sufficient information for structural seismic risk assessment at a specific site. In this case, a number of additional parameters, such as the soil resonance frequency or the whole shear-waves profile to the bedrock would be required. On the other hand, in the case of a large area of interest (i.e., large-scale/regional seismic risk analyses), because more refined soil information is often impossible to acquire, $V_{S,30}$ (or $V_{S,eq}$) values are commonly considered as viable parameters. Moreover, in these cases, since actual measurements are usually available at a limited number of sites, strategies to extend the single-site evaluations to a broader area are often required. Several approaches have been proposed in both technical and scientific literature (see for instance [32,33]) based on geological, geomorphological or geotechnical units [34–39]. Thompson et al. [40] proposed a $V_{S,30}$ map for the California using a hybrid geostatistical approach able to account for geology, topography, and site-specific shear-wave velocity measurements. Although there is extensive literature on the topic, the most widespread method, due to its user-friendliness, is the United States Geological Survey (USGS) approach developed in [41]. The method is based on the use of a correlation between topographic slope and $V_{S,30}$; according to that method, steep slopes generally reflect rock formations,

96 nearly-flat areas indicate soft soils and intermediate slopes correspond to stiff soils (the accuracy of
97 results often depends on the resolution of the digital elevation model). Lemoine et al. and Forte et al.
98 [42,43] compared the $V_{S,30}$ map predicted by USGS method for Mediterranean Europe and a case
99 study in Italy with a fair collection of V_S measurements. Both studies found that the USGS approach
100 tends to overestimate the actual $V_{S,30}$ measurements.
101 In Italy, site classifications on a national scale have been made by the Italian *Istituto Nazionale di*
102 *Geofisica e Vulcanologia* (INGV), which is responsible for providing the seismic hazard map for
103 structural design in Italy. More specifically, Luzi and Meroni [44] proposed a national 1:500.000 map
104 for site classification, based on a broad geological criterion considering lithology and age, and related
105 to three ground types. Later, Michelini et al. [45] upgraded this map by classifying the geological
106 units derived from the 1:100.000 geology map of Italy into five ground categories (from A to E).
107 They correlated these categories to those specified by EC8 (see the next section), being characterized
108 by the following reference $V_{S,30}$ values: (A) 1000 m/s; (B) 600 m/s; (C) 300 m/s; (D) 150 m/s; (E)
109 250 m/s, with soil thickness < 20 m. The most recent map was provided by Di Capua et al. [46] based
110 on 1:100.000 geological maps. It represents an attempt to merge geological formations in lithoseismic
111 classes following their lithological description, in order to identify areas characterized by a
112 homogeneous seismic response.
113 In the remaining part of the paper, a four-step procedure for correlating the surface geological maps
114 with site-specific investigations is presented. Then, referring to the Italian case, each step is
115 quantitatively described. An intermediate result of the procedure is the assessment of medians and
116 standard deviations of $V_{S,30}$ and $V_{S,eq}$ parameters for all the Italian sites. The final result is the soil
117 classification, according to EC8 and ItBC2018, of the country. All results are provided by means of
118 a software (available at http://wpage.unina.it/iuniervo/SSC-Italy.zip) that can be a useful tool for large
119 scale seismic studies or post-earthquake shakemap generation (e.g., [47,48]). Finally, an illustrative

120 application is carried out to quantify the effect of soil classification in the case of probabilistic seismic
121 hazard analysis at a national scale.

122 2. Methodology

123 From 2008 until the beginning of 2018, the [49] was the national seismic code for structural design
124 and assessment. Criteria for soil classification were in good accordance with the current version of
125 EC8. The latter associates a soil class on the basis of $V_{S,30}$ assessment or, alternatively, on the values
126 of SPT blow-count or the undrained shear strength of soil. The description of each soil class together
127 with the $V_{S,30}$ intervals are reported in Table 1 for the sake of completeness. The $V_{S,30}$ parameter could
128 be computed from the V_S profiles that are characterized by a gradual increase of mechanical properties
129 with depth. In the table, four main soil categories (from A to D) are identified for decreasing $V_{S,30}$
130 value. Then, three other classes (E, S1, S2) can be defined considering additional information.

131 **Table 1.** Ground type/Soil classification according to EC8.

Ground type/Soil class	Description of stratigraphic profile	$V_{S,30}$ [m/s]
A	Rock or other rock-like geological formation, including at most 5 m of weaker material at the surface.	> 800
B	Deposits of very dense sand, gravel, or very stiff clay, at least several tens of meters in thickness, characterized by a gradual increase of mechanical properties with depth.	800 – 360
C	Deep deposits of dense or medium-dense sand, gravel or stiff clay with thickness from several tens to many hundreds of meters.	360 – 180
D	Deposits of loose-to-medium cohesionless soil (with or without some soft cohesive layers), or of predominantly soft-to-firm cohesive soil.	< 180
E	A soil profile consisting of a surface alluvium layer with Vs values of type C or D and thickness varying between about 5 m and 20 m, underlain by stiffer material with Vs>800 m/s.	-
S1	Deposits consisting, or containing a layer at least 10 m thick, of soft clays/silts with a high plasticity index (PI>40) and high-water content.	< 100 (indicative)
S2	Deposits of liquefiable soils, of sensitive clays, or any other soil profile not included in types A – E or S1.	-

132

In the new version of the Italian building code, ItBC2018, some differences in the criteria for soil site classification have been introduced. Site classification now refers to $V_{S,eq}$, the number of soil classes has been reduced to five and the definition of class E has been changed as reported in Table 2.

Table 2. Ground type/Soil classification according to ItBC2018.

Ground type/Soil class	Description of stratigraphic profile	$V_{S,eq}$ [m/s]
A	Rock or other rock-like geological formation, including at most 3 m of weaker material at the surface.	> 800
B	Deposits of very dense sand, gravel, or very stiff clay, at least several tens of meters in thickness, characterized by a gradual increase of mechanical properties with depth.	800 – 360
C	Deep deposits of dense or medium-dense sand, gravel or stiff clay with thickness higher than 30 meters and characterized by a gradual increase of mechanical properties with depth.	360 – 180
D	Deposits of loose-to-medium cohesion soil with thickness higher than 30 meters and characterized by a gradual increase of mechanical properties with depth.	180 – 100
E	Soils with characteristics and equivalent shear velocity analogous to those defined for classes C and D but with a deposits thickness not higher than 30 meters.	-

This paper provides statistics of $V_{S,30}$ and $V_{S,eq}$ values for the Italian sites that are used to derive a seismic soil classification on a national scale according to both EC8 and ItBC2018. Here the general procedure adopted in the study is summarized. The approach aims to account for two types of information that are (i) the site-specific investigations and V_S measurements, and (ii) the existing geological maps that identify geographic area, or polygons, with homogeneous features. The procedure is summarized in four steps.

1. The first effort was the search and collection of the available data about investigations performed for any inland site of Italy. Retrieved information was analysed by the authors in order to obtain a dataset of geographical locations and soil classes. All data were stored in a geographical information system (GIS) database and, for each investigation, the values of $V_{S,30}$ and $V_{S,eq}$ were calculated.
2. Starting from the original geological formations as classified by *Istituto Superiore per la Protezione e la Ricerca Ambientale* (ISPRA), a simplified geo-lithological classification was

set up. The new classification accounts for similar lithology, geomorphologic setting, genetic processes (*facies*), age and seismic behavior of the original categories. The geo-lithological classification polygons were digitized and implemented in the GIS database.

3. Data from step one and step two were combined: values of $V_{S,30}$ and $V_{S,eq}$ were grouped as function of the geo-lithological class in which they were measured and the statistics were computed for each class.
4. Finally, V_S measurements were associated to each geo-lithological class, together with the first, second (median value) and third quartiles of the considered distributions. This allowed to provide $V_{S,30}$ and $V_{S,eq}$ median values and standard deviations for each geo-lithological complex. Additionally, as described in Section 6, combining the V_S measurements with the other available information, each investigated site was classified according to soil classes proposed by EC8 and ItBC2018. This allowed to identify a more probable soil class for each geo-lithological complex which has been assumed as representative of the complex.

It should be noted that two new contributions can be identified in the procedure. First, this is, to authors' knowledge, the first attempt to collect the available measurements of soil shear-wave velocities on a national scale in Italy, combined with geo-lithological characteristics. This requires a significant effort in the search and homogenization of information and allows continuous enrichment of the database with new available investigations. Second, the identification of geo-lithological complexes and the association of V_S statistics, as well as soil classes, to each complex have not been proposed before for Italy. Nevertheless, similar procedures were described in [37] and [43], which developed the maps for single Italian regions (Campania and Molise, respectively), using a smaller sample of V_S measurements.

3. Available data (step one)

The authors collected data from a wide range of sources resulting in a strongly uneven distribution in both quantity and quality of the information. This is mainly because only some Italian administrative regions operate geological services that collect and distribute data; consequently there are no common standards about the data and format. More specifically, data used in this paper were retrieved from the following sources (see the Data sources section for further details): available scientific and technical reports for the seismic characterization of the strong-motion stations of the Italian Accelerometric Archive (ITACA); reports from microzonation projects for the Abruzzo, Molise and Basilicata regions; regional databases of the seismic service of Emilia Romagna; Civil Protection studies for Sicilia and Trentino Alto-Adige regions; local site effects valuation Project for Toscana (VEL); local civil engineering practitioners; scientific reports; civil engineering projects and unpublished technical reports.

The collected data are considered reliable if the location is clearly defined and V_S is measured through standard geophysical tests. This implies, for example, that $V_{S,30}$ values inferred through the most common or recent empirical correlations with penetration resistance (e.g., [12,14,30]) were excluded. Moreover, in some cases, available data are characterized by shear-wave velocity profiles that do not reach 30 m; these data were not used to compute $V_{S,30}$ even if several methods allow to infer it from shallow velocity profiles (e.g., [50–52]). These same data were adopted only to compute $V_{S,eq}$ when the depth of the bedrock is known. Apart from shear-wave velocity measurements, a number of sites have other relevant information as geological description of the study area, stratigraphic logs, and results of laboratory and field geotechnical tests.

The available in situ tests were uploaded as a database (DB) in a GIS environment. The DB consists of an identifier code for the different regions of Italy, UTM geodetic coordinates, type of investigation, data source, the shear-wave velocity at each depth (when available), that is $V_{S,z}$, and

197 $V_{S,30}$ or $V_{S,eq}$ measurements. A detailed description of the database is reported in the following but,
198 before proceeding any further it is important to recall that the assessment of $V_{S,30}$ and $V_{S,eq}$ requires
199 slightly different information, hence data were differently selected depending on the considered
200 parameter.
201 The complete database features 3842 V_S measurements. In 16 cases, the $V_{S,z}$ profiles are extended to
202 the bedrock depth, which is shorter than 30 m; thus, they cannot be used for the $V_{S,30}$ assessment.
203 Therefore, two subsets of data of 3826 and 3842 measurements are used for $V_{S,30}$ and $V_{S,eq}$,
204 respectively. As pertaining to $V_{S,30}$, Table 3 describes the DB in detail: the measurements come from
205 different types of investigations: 1570 In-Hole Tests (DH, CH, SCPT), 319 Surface Geophysical
206 Tests (MASW, SASW, seismic refraction surveys) and 1937 Microtremors (ESAC, Re.Mi., HVSR,
207 Passive Array, FTAN) designed to measure shear-wave velocity profiles (ASTM D7400-08 [53]).
208 For each type of investigation, the table shows the available information. For 1433 sites, only the
209 $V_{S,30}$ value is available, whereas for 2393 sites the $V_{S,z}$ profile to 30 m depth is available; among these,
210 for 815 sites, the seismic bedrock is less than 30 m deep while in the remaining 1578 it is deeper than
211 30 m.
212 The location of the collected data in terms of type of investigation is reported in Figure 1. The figure
213 shows that the overall data distribution clearly follows the Apennine mountain chain, where there is
214 the largest seismic hazard [54], or identifies the areas affected by the most recent earthquakes (the
215 magnitude, or M, equal to 6, Umbria-Marche earthquake, 1997; the M5.7 Molise earthquake, 2002;
216 the M6.3 L'Aquila earthquake, 2009; the M6 Emilia sequence, 2012), where post-event studies
217 provided a relevant number of investigations. It should also be noted that Microtremors provide a less
218 accurate estimation of shear-wave velocity with respect to In-Hole Tests and Surface Geophysical
219 Tests. Although Microtremors provide the highest percentage of data (about 45%), these kinds of test
220 were concentrated in two regions: Emilia Romagna and Trentino Alto Adige. On the other hand, In-

221 Hole Tests, which provide the most accurate information, are distributed over a large area covering
222 the whole Apennine chain.
223
224 **Table 3.** Subset of data adopted for $V_{S,30}$.

Investigation type	Seismic bedrock deeper than 30 m	Seismic bedrock less deep than 30 m	Only $V_{S,30}$ available	Total number of data
In-Hole tests	607	903	60	1570
Surface Geophysical Tests	82	101	136	319
Microtremors	126	574	1237	1937
Total number of data	815	1578	1433	3826

225

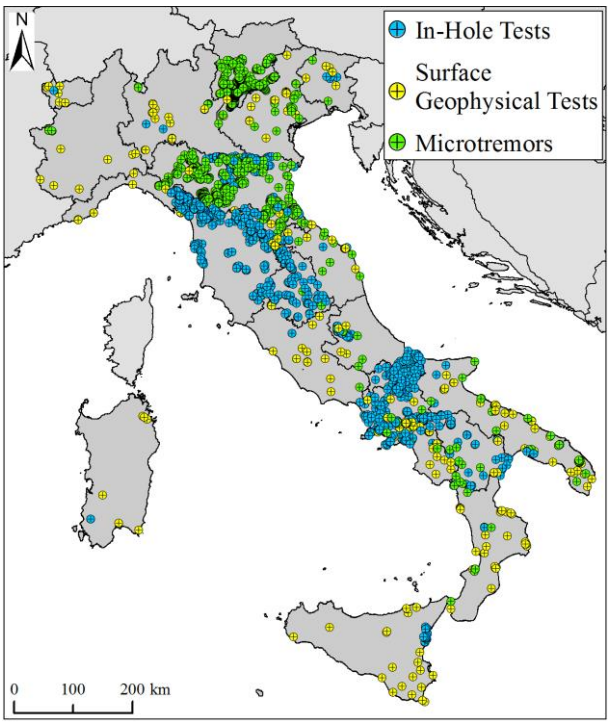

226
227 **Figure 1.** Distribution and type of collected data. .
228
229 The preliminary screening of data provides slightly different results when the $V_{S,eq}$ is considered. In
230 this case, investigations in which $V_{S,z}$ profiles reach the seismic bedrock can be used even if they do
231 not reach the depth of 30 meters (Table 4). Thus, a total of 3842 investigations are considered eligible
232 for $V_{S,eq}$ identification. Among them, 2409 are those in which the entire $V_{S,z}$ profile to the bedrock is
233 available (seismic bedrock is deeper than 30 m in 1578 sites whereas is less than 30 m deep in 831);

for the remaining 1433 sites only the $V_{S,30}$ is available. In these cases, to avoid rejecting a large amount of data, it is assumed that the seismic bedrock is deeper than 30 m and consequently $V_{S,30}$ is equal to $V_{S,eq}$.

Table 4. Subset of data adopted for $V_{S,eq}$.

Investigation type	**Seismic bedrock deeper than 30 m**	**Seismic bedrock less deep than 30 m**	**Only $V_{S,30}$ available**	**Total number of data**
In-Hole tests	622	903	60	1585
Surface Geophysical Tests	83	101	136	320
Microtremors	126	574	1237	1937
Total number of data	831	1578	1433	3842

A preliminary classification is performed as a function of velocity intervals for both considered parameters. Considered intervals are those used by EC8 and ItBC2018 for soil class identification, that is, >800 m/s, 800-360 m/s, 360-180 m/s and <180 m/s. Classification results are reported inFigure 2. According to the figure, most of the sites (51%) are in the 800-360 m/s interval of $V_{S,30}$, while the 38% are within 360-180 m/s. Fewer sites (5%) have $V_{S,30}$ higher than 800 m/s and 6% of sites are lower than 180 m/s. Similar are the results in terms of $V_{S,eq}$: 3% of sites are higher than 800 m/s, the majority (47%) are within 800-360 m/s, 44% are within 360-180 m/s and 6% are lower than 180 m/s. Site class A represents the seismic bedrock and is characterized by fewer investigations with respect to the others. This is due to the common practice of not performing geophysical investigations on rock outcrops (usually in mountainous settings). On the other hand, more efforts are usually addressed to the characterization of areas of towns or engineering works that, in Italy, mainly correspond to B and C soil classes.

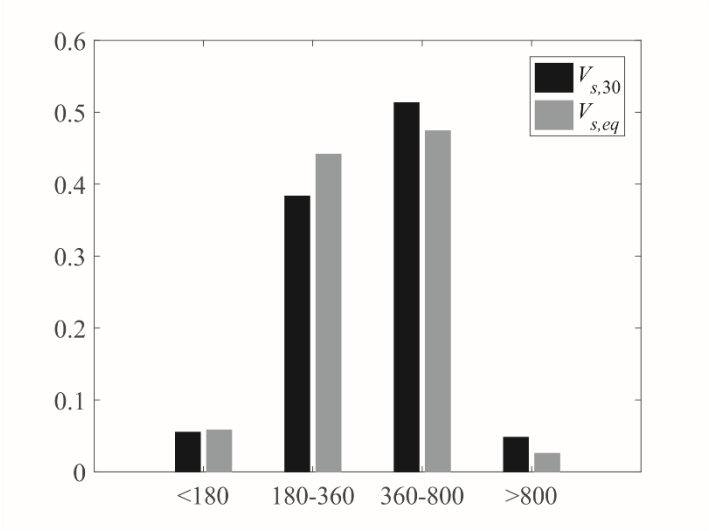

253

254 **Figure 2.** Distribution of data with respect to $V_{S,30}$ and $V_{S,eq}$.

255 ## 4. Geo-lithological map (step two)

256 ISPRA is currently building the geological map of Italy at a 1:50.000 scale. It will cover the national
257 territory with a total of 652 sheets but only 254 of them are available so far. Two hundred seventy-
258 seven geological maps covering Italian territory produced by ISPRA at the 1:100.000 scale [55] are
259 adopted for this study. They were completed in 1976 from field surveys performed on a 1:25.000
260 scale. Each geologic formation is characterized by lithological characteristics and age. However,
261 similarly to other geological classifications on a national scale (see for example [56], for the case of
262 Greece), it is easy to identify a lack of consistency at the boundaries of each sheet in which the
263 territory is divided. This is due to the different interpretations and classifications made by geologists
264 who carried out the survey in different years and adopting different classification criteria. In order to
265 combine these national geological maps with the data described in the previous section, a simplified
266 classification harmonizing the original categories was set up, involving expert judgement.
267 With this aim, broader categories were introduced as function of similar lithology and
268 geomorphologic setting, genetic processes (*facies*), age, and seismic behavior. To give an example,
269 all the original geological formations described as "gravel and sand coming from river and alluvial
270 environment" were grouped, because these types of soil have, in general, very similar lithological

features independently of the geographic location. Other examples are some geologic bedrocks such as "limestones" or "crystalline rocks".

In fact, a relevant distinction was based on the identification of geo-lithological complexes as *geologic bedrock* (Paleozoic to Pleistocene) versus those representative of *cover deposits* (Quaternary). Geologic bedrock formations were mainly grouped from a lithological and age point of view (note that geologic bedrock category is not directly related to defined values of V_S), while cover deposits were distinguished by depositional environment, also accounting for soil grain categories, as it is a general understanding that V_S values increase passing from fine-grained soils to coarser ones. The followed approach permitted to summarize the Italian geological setting in eighteen geo-lithological complexes. Furthermore, an effort to better characterize some local Italian geological features can be found in the distinction in two different sub-complexes for Igneous metamorphic bedrock (IMB) and Lava bedrock (LB). Indeed, some Italian geographic areas experienced a different tectonic history, which strongly modified the fracturing states and resulted in the IMB1 and IMB2 sub-complexes. Meanwhile, LB1 and LB2 are characterized by a different magmatic composition, which strongly controlled the eruptive style and the consequent deposits [57]. These issues could affect the soil properties and the geo-lithological complexes considered hereafter are twenty. Each of them is described in Table 5, while the map representing the twenty identified complexes is reported in Figure 3.

Table 5. Geo-lithological complexes

Name of the Complex	**ID**	**Description**	**Geologic Age**
Cover deposits			
Pyroclastic soil deposits	**pyr**	Successions of Ashes, Pumices and Scoriae	Pleistocene-Holocene
Tuff and scoriae deposits	**tfs**	Tuffs and Ignimbrites	Oligocene - Pleistocene
Clay silt and peat deposits	**csp**	Clays, Silts, Peat from palustrine environment	Pleistocene-Holocene
Sand deposits	**sd**	Sands and Gravels from Dunes and Beaches	Pleistocene-Holocene
Gravel and sand deposits	**gs**	Conglomerates, Gravels and Sands from alluvial deposits.	Pleistocene-Holocene
Terraced conglomerate deposits	**tcg**	Conglomerates, Sands and Shale from terraced successions.	Pleistocene

Shallow debris deposits	**db**	Infill, Alluvial fan, Debris, Colluvium, Breccia, Debris talus and Sandy-silt talus on igneous and metamorphic bedrock.	Pleistocene-Holocene
Moraine deposits	**mr**	Moraines deposits and large landslide bodies	Pleistocene
Travertine deposits	**tv**	Travertines and soft limestones	Pleistocene-Holocene
Geologic Bedrock			
Lava bedrock	**LB1**	Porphyries and Lava	Paleozoic - Holocene
	LB2	Lava (Sardinia and Sicily)	Pleistocene - Holocene
Sand bedrock	**SB**	Sands and sandstone bedrock	Pliocene - Pleistocene
Conglomerate bedrock	**CgB**	Gravels and conglomerates bedrock	Pliocene -Pleistocene
Clay flysch bedrock	**CFB**	Clayey Flysch, phyllites, clayey schists	Cenozoic - Pleistocene
Arenaceous flysch bedrock	**AFB**	Arenaceous and marly flysch, marly limestones, gypsums, clayey metamorphic rocks	Cenozoic
Marly calcareous bedrock	**McB**	Calcareous successions deposited in basin environment	Meso-Cenozoic
Calcareous tuff bedrock	**CtB**	Calcareous sandstones	Pliocene - Pleistocene
Carbonate bedrock	**CB**	Limestones, Dolostones, Marbles	Meso - Cenozoic
Igneous metamorphic bedrock	**IMB1**	Igneous and metamorphic rocks (Sardegna, Lombardia; Valle d'Aosta, Toscana)	Paleozoic - Cenozoic
	IMB2	Igneous and metamorphic rocks (Calabria, Sicilia, Liguria)	Meso- Cenozoic

291

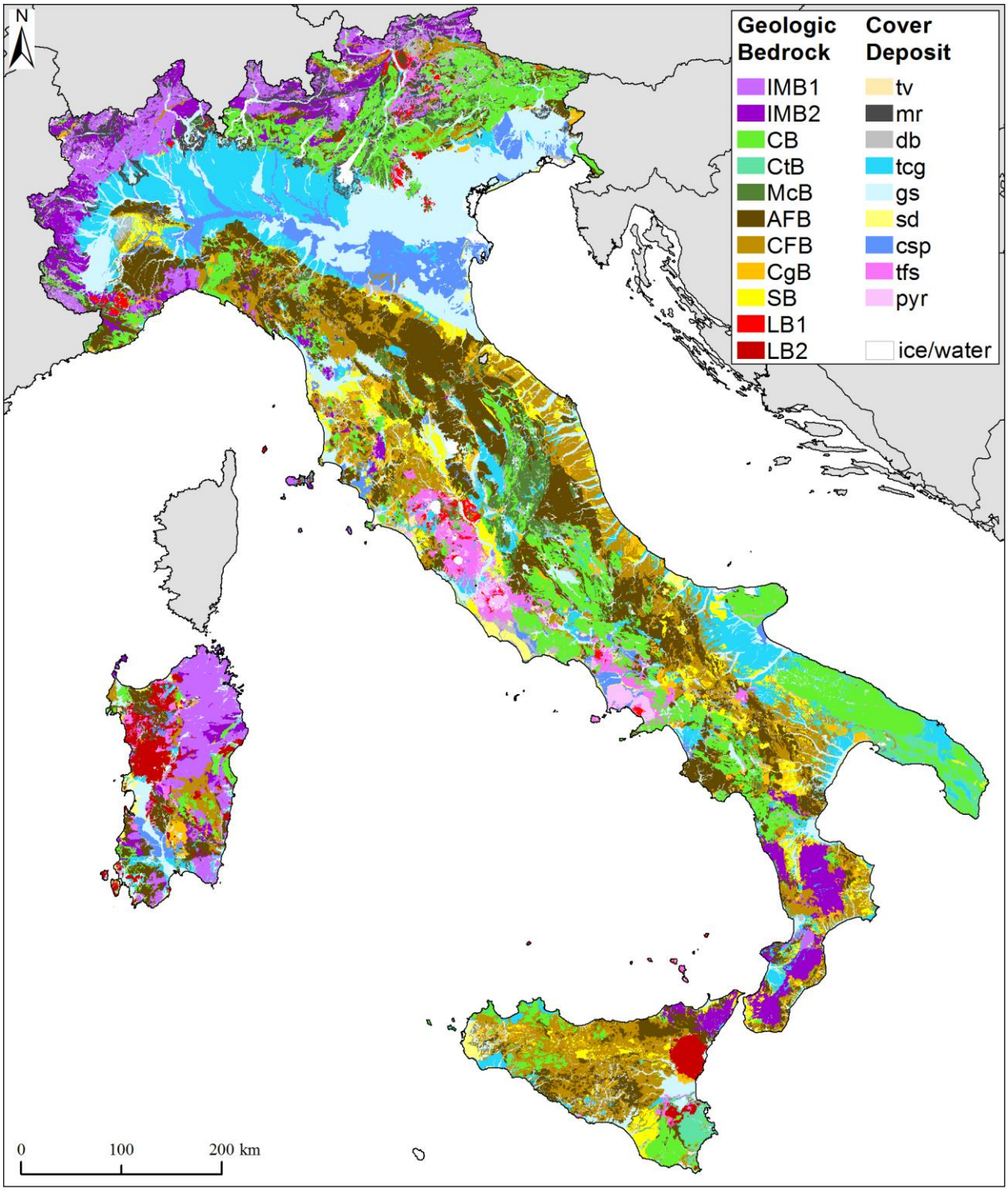

Figure 3. Map of Italy showing the identified geo-lithological complexes (keys in Table 5). Ice or water are reported in white.

The identified complexes account for the overall geological formations existing in Italy; however, an analogous classification could be adopted in other countries, as all geological materials and environments identified in this classification can also be found worldwide.

5. Statistics of Vs values per geo-lithological complex (step three)

The $V_{S,30}$ and $V_{S,eq}$ measurements are grouped into the twenty geo-lithological complexes shown in Table 5. The statistics of $V_{S,30}$ data associated to each complex are computed and represented through the box-plots of Figure 4 (numerical values of mean, median and standard deviations of data are reported in Appendix). In the same figure, the number of data for each geo-lithological complex are also shown (data in IMB1 are few and first and second quartiles cannot be graphically distinguished).

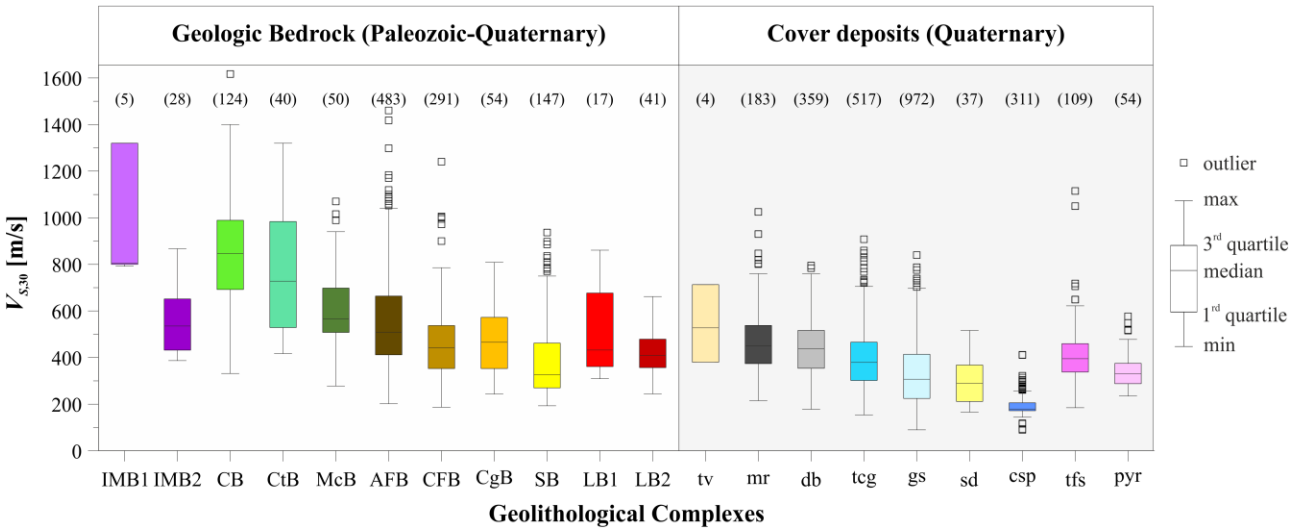

Figure 4. Box-plots showing the distributions of $V_{S,30}$ for the geo-lithological complexes listed in Table 5.

The first, second (median value), and third quartiles are reported together with the minimum and maximum values of the empirical distribution. The outliers are defined as the values that lie outside the range defined by 1.5 times the interquartile range (IQR) minus the first quartile and 1.5 times the IQR plus the third quartile (e.g., [58]).

For the geologic bedrock formations, Figure 4 shows that the distinction between the two sub-complex IMB1 and IMB2 resulted in differences of soil characteristics: median $V_{S,30}$ values are 805 m/s and 536 m/s, respectively. On the other hand, median values associated to LB1 and LB2 are almost equal (some differences between LB1 and LB2 appear when $V_{S,eq}$ is of concern, as shown in Figure 5). All the other geologic bedrock complexes resulted in median $V_{S,30}$ between 360 and 800 m/s, with the exception of CB and SB, which have median value equal to 847 and 326 m/s, respectively. For Quaternary deposits, Figure 4 shows that they are characterized by shear-waves velocity clearly decreasing as function of the grain-sizes, sorting and textures. Coarse gravel-grained and massive deposits, such as tv, mr, db and tcg, resulted in median $V_{S,30}$ between 360 and 800 m/s, finer deposits made of gravels and sands resulted within 180 and 360 m/s (gs, sd), while $V_{S,30}$ lower than 180 m/s was attributed to silts, clays and peats grouped in the csp complex. Finally, the distinction between ignimbrites (tfs) and pyroclastic soils (pyr), with the former being more lithic and the latter loose, resulted in two different intervals of $V_{S,30}$: between 360 and 800 m/s and 180 and 360 m/s, respectively.

An analogous classification is performed with respect to $V_{S,eq}$, as reported in Figure 5. Results are in good accordance with those shown in the previous figure. The only differences are: (i) LB2 does not belong to the 360 – 800 m/s interval, having median value of 315 m/s; (ii) IMB2 has median value lower than 800 m/s and equal to 476 m/s. The latter are due to the definition of $V_{S,eq}$, which does not take in account the increase of stiffness provided by the seismic bedrock contribution.

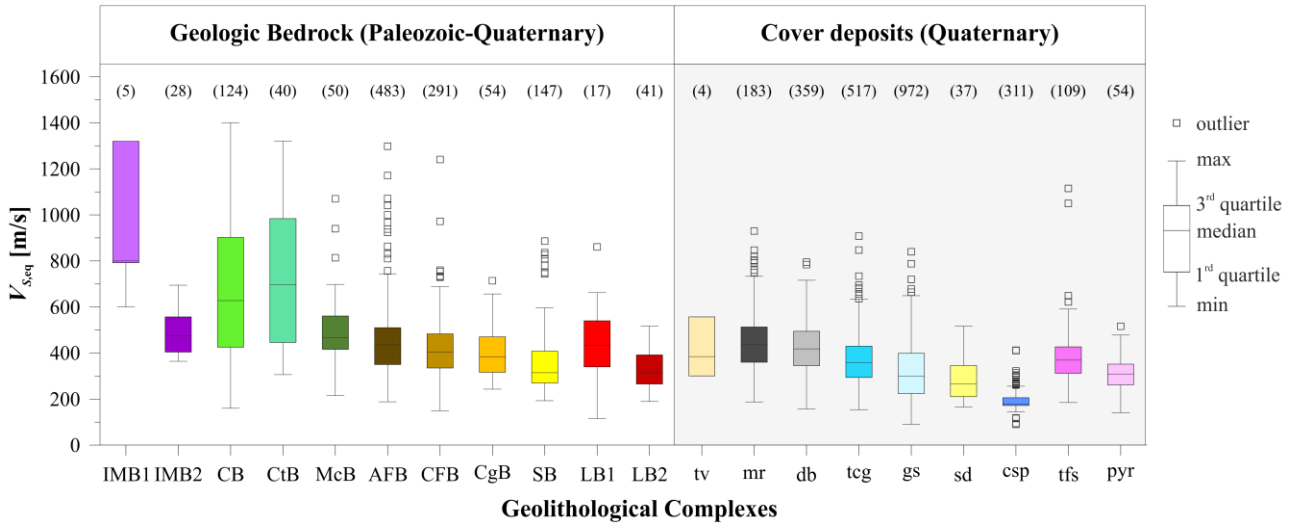

Figure 5. Box-plots showing the distributions of $V_{S,eq}$ values measured by geophysical tests, in the geo-lithological complexes listed in Table 5.

6. Seismic soil classification of Italian sites (step four)

In the framework of this study, median and standard deviation values of $V_{S,30}$ and $V_{S,eq}$ of each geo-lithological complex are associated to all locations within a complex. This allows providing a soil characterization for the whole national territory that can be used in the case of large-scale seismic hazard/risk analysis.

Figure 6 shows the maps of (a) $V_{S,30}$ and (b) $V_{S,eq}$ distribution for Italy coming from the median values identified from the box-plots of Figure 4 and Figure 5, respectively. The two maps display a similar shear-waves velocity distribution, with some differences for the values higher than 800 m/s, which are more present in Figure 6a and the 180 – 360 m/s range, which in Figure 6b replaces some sites identified in the range 360 – 800 m/s in Figure 6a.

Figure 6c reports the corresponding $V_{S,30}$ map of [45] for comparison. It shows a widespread distribution of sites characterized by values higher than 800 m/s, with fewer areas in the range 360 – 800 m/s. The sites having 180 – 360 m/s values are mainly concentrated in the North, while values less than 180 m/s are poorly represented.

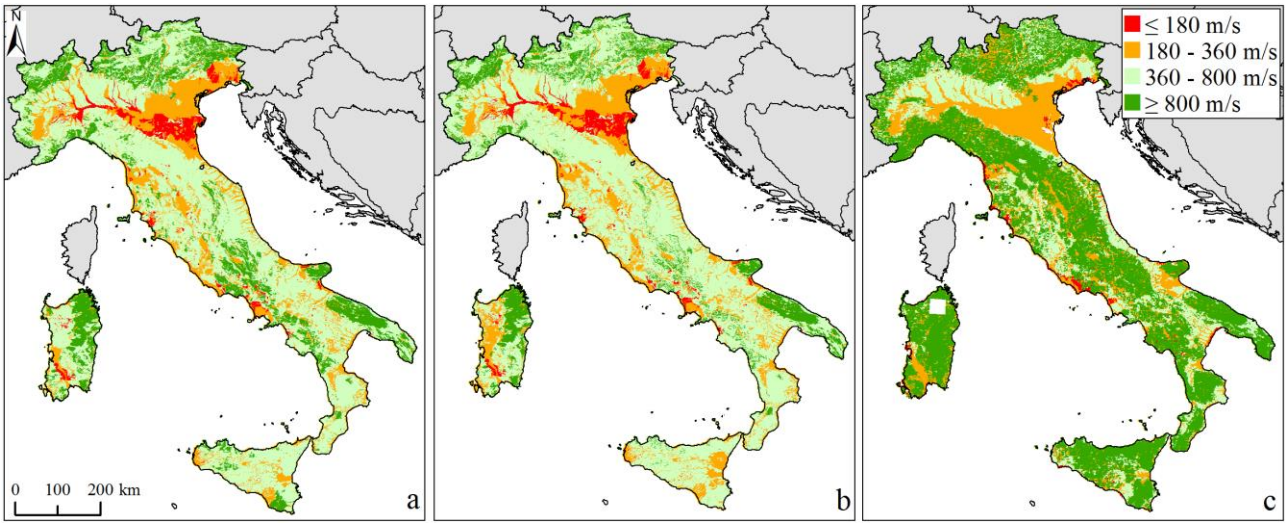

Figure 6. Maps of shear-wave velocity for Italy: (a) and (b) median values of $V_{S,30}$ and $V_{S,eq}$, respectively, according to this study; (c) map of $V_{S,30}$ provided by [45].

Recall (Table 1 and Table 2) that both EC8 and ItBC2018 classifications account for some soil classes that are not defined exclusively on the basis of V_S measurements: these are class E, S1 and S2 for EC8 and class E for ItBC2018. Hence, some additional analyses of data are required to extend soil classification to code-conforming classes. More specifically, after having grouped data per geo-lithological complex, each site is classified in accordance with EC8 and ItBC2018. Thus, the frequency of soil class occurrence for each complex is computed and the most frequent (modal) soil class is assumed as the representative class of the whole complex.

According to this procedure, Figure 7 shows the soil class frequencies in accordance with EC8 classification. In most cases, one soil class is predominant with respect to the others, but for CB and CtB the frequencies of A and B class occurrences are comparable, and for tcg and csp frequencies of B and C class occurrences are comparable.

Comparing Figure 4 and Figure 7, it can be seen that site classification of the latter is in perfect accordance with the median $V_{S,30}$ values shown in the former. This is partially described by the fact that the number of investigations that assigned class E (the soil class not defined only on $V_{S,30}$ parameter) is negligible.

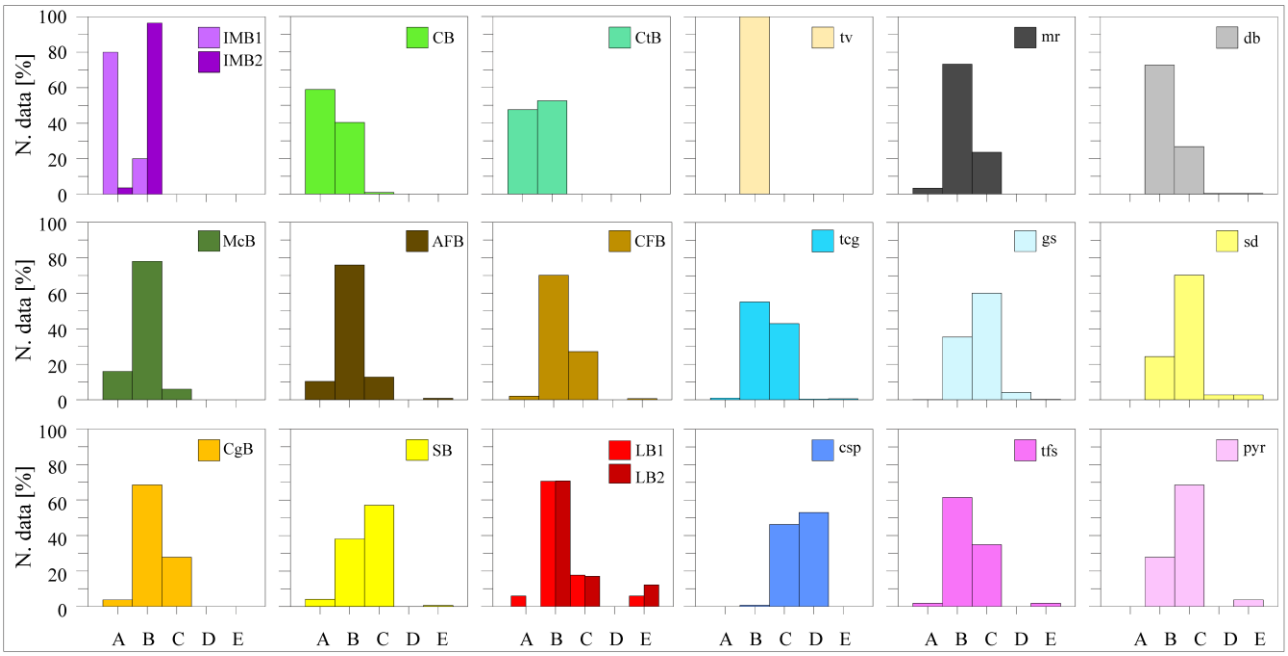

Figure 7. Histograms showing the distributions of soil classes according to EC8 for each geo-lithological complex listed in Table 5.

Soil class frequencies in accordance with ItBC2018 classification are reported in Figure 8. For each complex, soil class attribution is the same as for EC8, except for LB2 and CB. Both these complexes display a significant presence of E site-class. Thus, an attempt to distinguish different local settings within the same complex is carried out. Topographic slope was assumed as a proxy for the identification of sub-areas. In particular, a value of 20° was considered representative of the critical slope value, above which only thin soils can bury a shallow bedrock, while areas characterized by slope less than 20° can accumulate thicker soils (e.g., [59]). Following this assumption, LB2 was classified as B and E, the former with slopes higher than 20° and the latter less than 20°. For complex CB, B class is the most frequent, although the analysis of data clearly shows that this complex is characterized by rigid materials, as the sum of A and E classes is greater than class B. These data are also biased by the fact that few investigations are performed on outcrops that are clearly bedrock, hence this complex was also split into sub-areas following the slope proxy, assuming E class where slope is lower than 20°, but assigning A to the slopes higher than 20°.

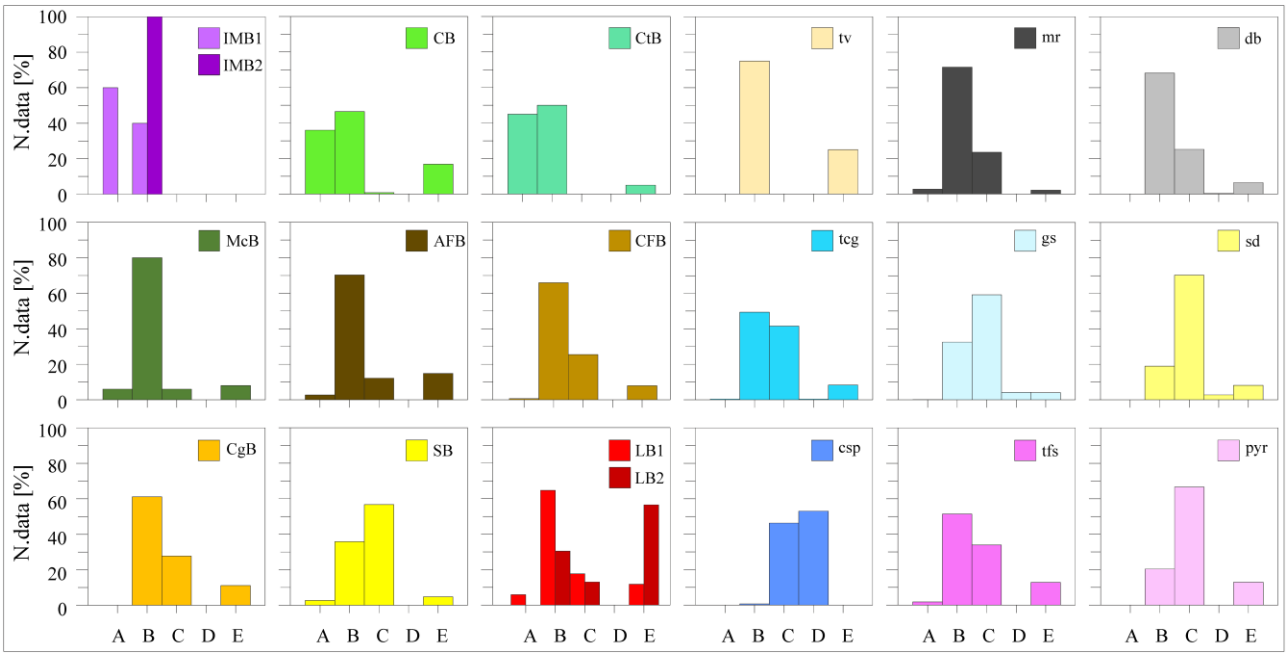

Figure 8. Histograms showing the distributions of soil classes according to ItBC2018 for each geo-lithological complex listed in Table 5.

7. Discussion

The code-conforming soil classes are attributed to the polygons of the geo-lithological map as shown in Figure 9a and Figure 9b for EC8 and ItBC2018 soil classes, respectively.

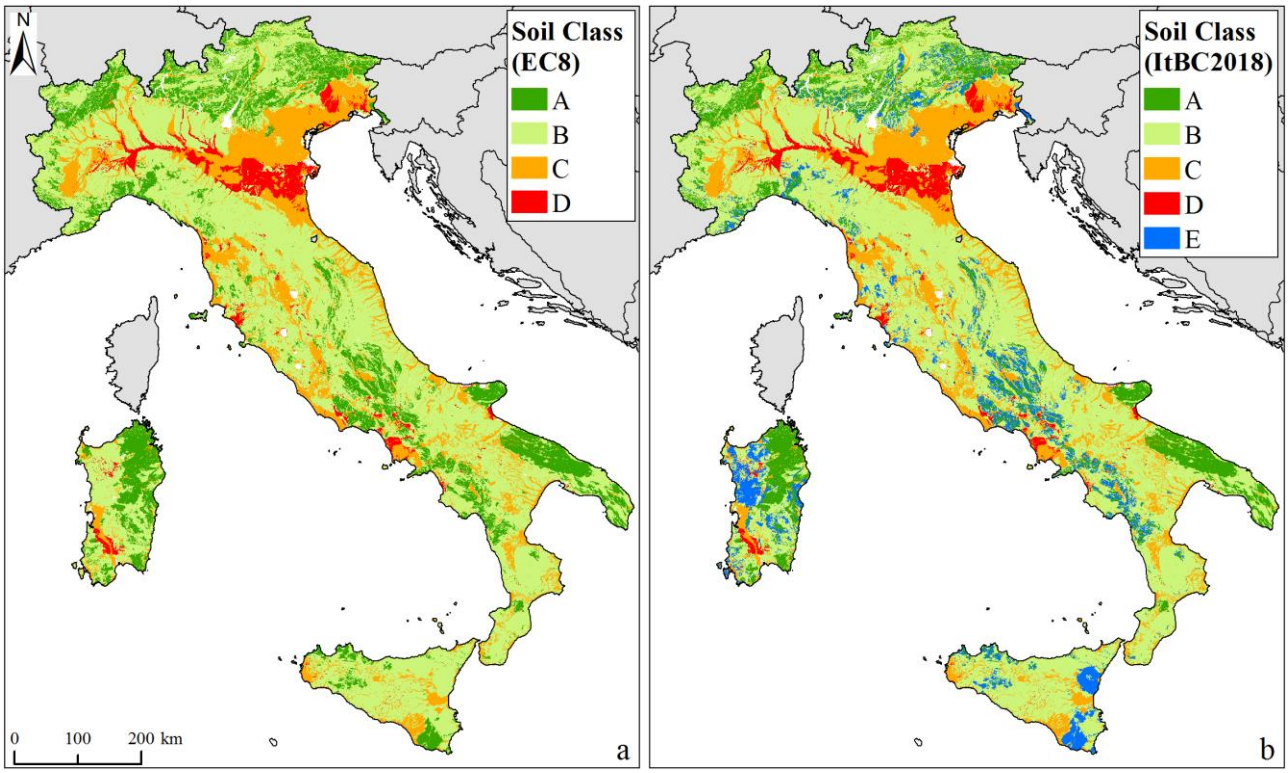

Figure 9. Soil Class maps obtained in accordance with (a) EC8 and (b) ItBC2018. Ice or water are reported in white.

Both maps provide, based on a 1:100.000 geologic scale, the seismic soil classifications suitable for large scale studies for which ground motion modifications due to stratigraphic amplification need to be accounted for. At this scale, a reasonable agreement can be observed between both maps, with an enhancement in the ItBC2018 maps, where the area characterized by E class is identified.

The EC8 map highlights a widespread B class distribution (57.4% of the area of Italy), followed by C (19.2%). The soil class A is 18.4% of Italian sites, D is the smallest area (4.2%), E class is not represented. On the ItBC2018 map, B is again the most represented (55.8%), A is lower (13.2%), C and D respectively remain 19.2% and 4.2%, while E class is characterized by 6.8%. In both the EC8 and ItBC2018 maps there are small areas (0.8%) which are not included in any of the soil classes, being representative of ice or water.

In order to discuss the global accuracy of classification, each measured soil class is compared with the inferred soil class of the polygon in which the measurement is enclosed. When the measured class

410 is less stiff than the soil class inferred from the polygon, the site is considered as “overestimated”
411 whereas it is considered as “underestimated” and “matched” when the measured one is stiffer than or
412 equal to the inferred class, respectively (Figure 10). It can be observed that mismatched values are
413 evenly distributed and local spatially coherent anomalies cannot be identified. Matched sites are the
414 63% and 60% of the total available measurements for EC8 and ItBC2018, respectively. The
415 overestimation is for 19% and 23% of the sites, whereas an underestimation is for 18% and 17% of
416 the sites with respect to EC8 and ItBC2018 classification, respectively.

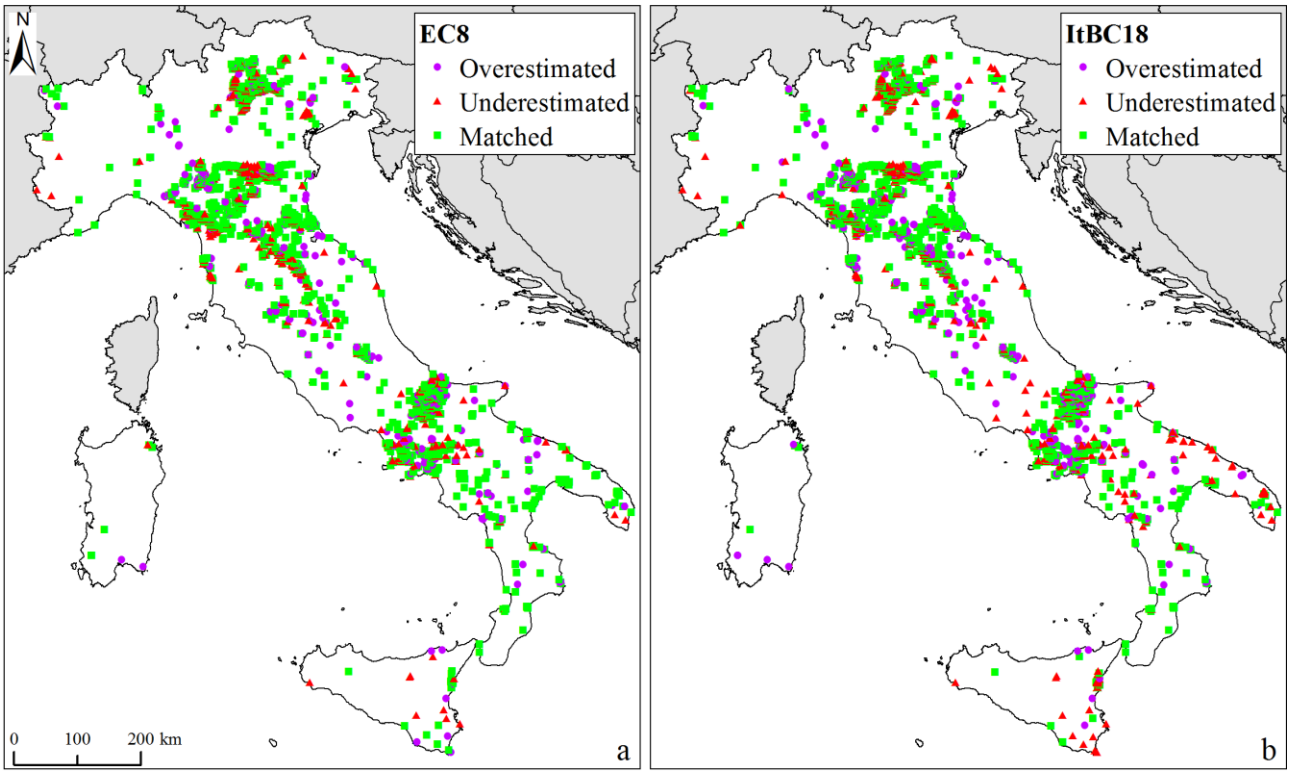

417

418 **Figure 10.** Geographic distribution of comparison between measured and inferred site classes
419 according to (a) EC8 and (b) ItBC2018.

420

421 A more quantitative discussion of EC8 results is provided through Table 6. Each line of the table
422 shows, for each measured soil class, the percentage of sites that are associated to each soil class in
423 the framework of this paper. For example, of the measured soil class A, 39.7% of sites are enclosed
424 into polygons corresponding to site class A in Figure 9a, 53.2% are enclosed into site class B and
425 7.1% are in site class C. Thus, 60.3% of the investigated sites from soil class A are underestimated

according to the polygons in Figure 9a. The second line of the table shows that the 71.3% of the total sites classified as soil class B by measurements are equivalently classified by the proposed procedure, while 3.9% and 24.7% are overestimated and underestimated, respectively. Indeed, B and D sites are the best predicted, with 78.6% correctly matched D class. As pertains to C class, half of the cases are correctly predicted (50.0%), while 40.0% are overestimated against 10% of underestimated. Finally, E class is never identified in the proposed procedure and most of investigations sites are attributed to B class (see Figure 7).

Table 6. Comparison between the inferred and the measured classes according to EC8

		Inferred Classes according to EC8 [%]				
		A	B	C	D	E
Measured classes	A	39.7	53.2	7.1	0.0	0.0
	B	3.9	71.3	24.7	0.1	0.0
	C	0.4	39.6	50.0	10.0	0.0
	D	0.0	1.4	20.0	78.6	0.0
	E	0.0	75.0	25.0	0.0	0.0

Similarly, Table 7 compares investigations with the soil class map according to ItBC2018. The results are quite similar for B, C, and D classes. E class is also represented; it results correctly matched for 13.8% of cases and it is mainly predicted as B. The A class still results in a poor-quality prediction with only 33.3% of sites correctly matched and 13.1% of cases falling in the E class.

Table 7. Comparison between the inferred and the measured classes according to ItBC2018

		Inferred Classes according to ItBC2018 [%]				
		A	B	C	D	E
Measured classes s	A	33.3	46.5	7.1	0.0	13.1
	B	2.4	70.2	24.4	0.2	2.8
	C	0.3	38.4	50.6	10.1	0.6
	D	0.0	1.4	20.0	78.6	0.0
	E	3.0	61.6	21.5	0.0	13.9

Finally, results are also discussed in terms of V_S statistics per soil class. To this aim, the measured data are grouped as a function of the EC8 soil class resulting from the discussed procedure (Figure

9a): the number of observations (N. of data), median, standard deviation and coefficient of variation (CV), that is the ratio of the standard deviation to the mean, of each group of data are reported in Table 8. The table shows a good accordance of median values with the interval identified by EC8 for each soil class (see Table 1). Dispersions of data are not negligible: site class B and C are those with the highest CV and are the classes in which the highest number of observations are located (2176 and 1210, respectively). The lowest number of observations (129) are within site class A and the CV is 0.26 while observations that are comprised in site class D are 311 and the corresponding dispersion of measurements is the lowest, i.e., 0.21; this is because only csp complex is associated to class D.

Table 8. Statistics of $V_{S,30}$ measurements for each soil EC8 soil class

	$V_{S,30}$ [m/s]			
	N. of data	Median	Standard deviation	CV
A	129	841	222	0.26
B	2176	444	170	0.36
C	1210	310	133	0.39
D	311	179	40	0.21

The equivalent analysis of results is reported in Table 9 referring to $V_{S,eq}$ and the ItBC2018 classification. Median values of measurements located in site classes from A to D are in good accordance with the reference code (see Table 2) whereas measurements pertaining to site class E are higher than what is expected, that is higher than the 100 - 360 m/s interval. Indeed, as discussed in Section 6, soil class E is identified in the LB2 and CB complexes by introducing the topographic slope as a proxy of the soil characteristics; Table 9 suggested that this strategy can be improved in future development of this work. The CV of B, C and D class are comparable with those of Table 8 while the CV of site class A is higher than the one associated to EC8 soil class.

Table 9. Statistics of $V_{S,\mathrm{eq}}$ measurements for each soil ItBC2018 soil class

	$V_{S,\mathrm{eq}}$ [m/s]			
	N. of data	Median	Standard deviation	CV
A	60	831	292	0.36

B	2141	405	145	0.34
C	1214	302	114	0.35
D	311	179	40	0.21
E	116	403	239	0.51

464

465 ## 8. Software for data retrieval and illustrative application

466 To make soil classification available to practitioners, a stand-alone software for database interrogation
467 was developed. It is named Seismic Soil Class-Italy (SSC-Italy) and provides the results of soil
468 classification for any set of sites within the inland Italian country. The tool is coded in
469 MATHWORKS-Matlab® and benefits from the graphical user interface (GUI) shown in Figure 11.
470 As first step, the user is required to select the reference code; i.e. EC8 or ItBC2018 (the selected code
471 can be modified at any step of the analysis). In the second step, the user defines the coordinates of
472 the site(s). For each selected site, SSC-Italy provides the corresponding soil class according to the
473 selected code. In addition, various forms of output can be exported: these are the map with the location
474 of the site(s) and a text file with the median(s) and the standard deviation(s) of $V_{S,30}$ (or $V_{S,eq}$) of the
475 polygon(s) containing the site(s), together with the geo-lithological complex(es) the point(s) belongs
476 to.

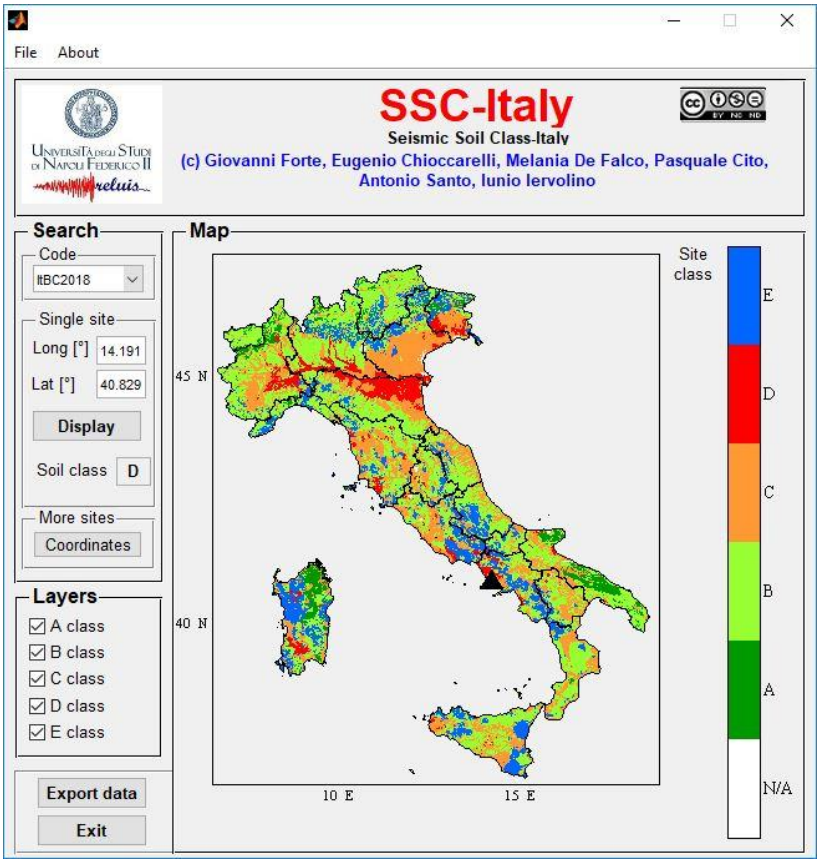

Figure 11. Main GUI of SSC-Italy software

8.1 Rock vs soil probabilistic seismic hazard in Italy

In this section, the importance of soil classification in regional analyses is highlighted via a large-scale application. To this aim, the peak ground acceleration (PGA) resulting from probabilistic seismic hazard analysis (PSHA, e.g. [60]) on a national scale and characterized by an exceedance return period (T_R) equal to 475 years, is computed accounting for the $V_{S,30}$ polygons derived in this paper. PSHA is performed adopting the same models as the official seismic hazard map used for design (which is provided for rock site conditions only), as described in [54]. The latter features a logic tree made of several branches and, among them, the branch named 921, in which the Ambraseys et al. [61] GMPE is considered. This branch produces the results that are considered to be the closest to those provided by the full logic tree. The seismic source model is the one of [62] which features 36 seismic source zones. For each zone, the annual rates of earthquakes belonging to discrete bins of

magnitude, that is *activity rates*, are adopted (see [63] for further details). A grid of about ten-thousand points covering the whole territory has been created and, at each site of the grid, the soil class from SSC-Italy is associated. Calculations are carried out with the REASSESS software [64]. Each site is classified in four classes of seismicity as a function of the resulting PGA values, between 0 and 0.1g, 0.1g and 0.2g, 0.2g and 0.3g, 0.3g and 0.4g.

The described analysis is then repeated assuming rock conditions for all the sites in order to compare the resulting seismicity classes. The maps for comparison are given in Figure 12 together with the seismic sources of [62]. For rock site conditions (Figure 12a), the first class includes the 33.2% of the sites, while 48.7% and 18.1% of the sites are obtained for the second and third hazard classes, respectively. Since the maximum PGA value on rock across Italy is equal to 0.27g, no sites can be found in the fourth seismicity class. Due to the soil effects (Figure 12b), the percentage of sites within the first and second class reduces to 23.2% and 37.4%, respectively. The sites with PGA in the range between 0.2g and 0.3g cover the 31.8% of the territory and, in the remaining 7.6% of sites, accelerations are between 0.3g and 0.4g. For each site, the soil effect on the seismic hazard assessment has also been computed as the *relative difference*, i.e., difference between the PGA considering the soil class and the PGA computed on rock divided by the PGA on rock. Then, for each class of seismicity on rock, the mean of relative difference has been evaluated. Such a mean difference does not vary significantly from one class to another, being equal to 24.8%, 27.5% and 25.6% for the first, second and third, respectively. This is expected because soil and seismic classes are independent and thus the soil effect on the hazard is uniformly spread on the seismic classes.

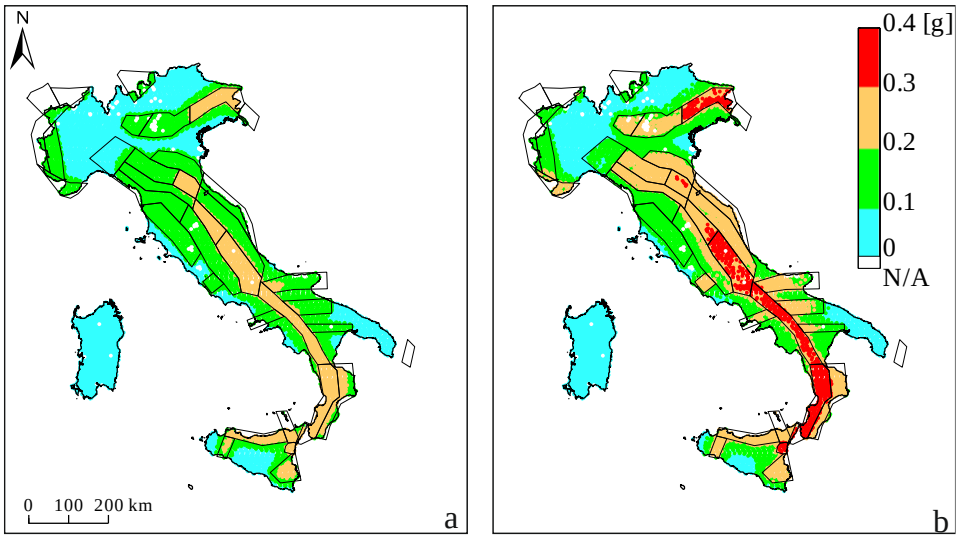

Figure 12. Seismic classification for Italy on (a) rock and (b) soil site condition; the sites in which the PGA is not assigned (N/A) are those belonging to the ice/water category of Figure 3

9. Conclusions

The study discussed in this paper addresses the issue of soil classification in Italy, which may be required, for example, for large scale seismic risk analyses or post-earthquake shakemap generation. In these cases, although site-specific seismic propagation analyses are not feasible, an approximate characterization of soil dynamic behaviour is required. The latter, which may be represented by the knowledge of $V_{S,30}$ or $V_{S,eq}$ is usually not available. On the other hand, large-scale geological maps are often available, but they do not include appropriate information for soil characterization in seismic conditions.

In the study, a four-step procedure to correlate the surface geological maps with site-specific investigations was presented and discussed. It was implemented for Italy, where geological maps at 1:100.000 scale are available, together with a large database of site specific investigations that were collected. The results, which can be upgraded as new site specific investigations become available, are maps of soil characteristics in terms of median and standard deviation $V_{S,30}$ and $V_{S,eq}$ values as

well as soil classification according to EC8 and ItBC2018. They have been made available through a simple stand-alone software (SSC-Italy) available at http://wpage.unina.it/iuniervo/SSC-Italy.zip.

The soil classes measured via site-specific investigations have been compared to the soil classes inferred from the maps. For EC8, in the 63% of sites the soil class is correctly matched whereas in 19% and 18% of cases soil classes are underestimated and overestimated, respectively. Similar percentages are obtained for ItBC2018 classification: 60% of sites are correctly matched, 23% are underestimated and 17% are overestimated.

To assess the effect of soil classification on a national scale, an illustrative application has been developed. It is the seismic hazard map of Italy in terms of PGA with 475-years return period on soil compared to the corresponding seismic hazard map computed for rock. Due to models adopted for computation, the latter is a good approximation of the national official seismic hazard.

It is important to finally remark that the derived results are not appropriate at all for site-specific studies as they do not replace microzonation and local site response studies, which require more detailed investigations for the soil site characterization and the structural design.

Appendix

Figure 4 and Figure 5 summarize data distribution for each geo-lithological complex. The numerical value of mean, median and standard deviation of data for each complex are reported in the following table in term of $V_{S,30}$ and $V_{S,eq}$.

Table A.

	$V_{S,30}$ [m/s]			$V_{S,eq}$ [m/s]		
Acronym	Mean	Median	Standard deviation	Mean	Median	Standard deviation
IMB1	981	805	254	863	800	269
IMB2	556	536	132	490	476	92
CB	855	847	221	670	628	302
CtB	777	728	253	741	697	287
McB	612	566	178	494	467	156
AFB	550	509	195	451	436	155

CFB	458	442	150	416	403	124
CgB	474	466	148	401	383	100
SB	384	326	168	355	315	133
LB1	511	432	172	439	432	177
LB2	419	409	84	329	315	80
tv	537	528	138	407	384	108
mr	465	451	141	455	436	138
db	441	439	120	424	418	117
tcg	396	379	132	367	360	108
gs	333	308	129	320	300	112
sd	296	290	96	284	267	89
csp	195	179	40	195	179	40
tfs	418	395	138	385	369	131
pyr	346	331	83	317	309	77

Data sources

- In addition to the cited references, data used in this study were readily accessible from the following sources (last accessed 18/09/2018):
- Italian accelerometric archive ITACA (http://itaca.mi.ingv.it);
- Seismic microzonation of Abruzzo Region (https://protezionecivile.regione.abruzzo.it/index.php/microzonazione);
- Seismic microzonation of Basilicata Region (http://www.crisbasilicata.it/microzonazione/index.html);
- Regional Seismological and Geological Service of Emilia Romagna Region (http://geo.regione.emilia-romagna.it/geocatalogo/);
- Regional Seismological and Geological Service of Molise Region (http://www3.regione.molise.it/flex/cm/pages/ServeBLOB.php/L/IT/IDPagina/381);
- Civil Protection of Catania for Sicilia Region (http://sit.protezionecivilesicilia.it/opcm3278/);
- VEL project for Toscana Region (http://www.regione.toscana.it/-/banca-dati-vel);

- Civil Protection of Trento for Trentino Alto-Adige (http://www.protezionecivile.tn.it/);
- Regional Seismological and Geological Service of Umbria Region (http://storicizzati.territorio.regione.umbria.it/Static/IndaginiGeologicheKmz/Index_kmz.htm);

Funding: This research was funded by the Italian Civil Protection Department RELUIS project 2010 – 2013, RS2 Task 2.1, 2.2 "Definition of geological models and site amplification for impulsive earthquakes near-source". The opinions and conclusions presented by the authors do not necessarily reflect those of the funding entity.

Acknowledgements: The authors acknowledge dr. Giovanni Lanzano and the other anonymous reviewers, whose comments and suggestions permitted to improve the overall manuscript. Grateful acknowledgments are due to dr. Giuseppe Di Crescenzo for the fruitful scientific contribution provided in the early stage of this research. Moreover, dr. Georgios Baltzopoulos is gratefully acknowledged for proofreading the manuscript.

References

[1] Kramer SL. Geotechnical earthquake engineering. Upper Saddle River, New Jersey 07458: Prentice-Hall, Inc.; 1996.

[2] Dobry R, Vucetic M. International symposium of geotechnical engineering of soft soils. Dyn. Prop. Seism. response soft clay Depos., 1987, p. 51–87.

[3] Seed RB, Dickenson SE, Idriss IM. Principal geotechnical aspects of the 1989 Loma Prieta earthquake. Soils Found 1991;31:1–26. doi:10.3208/sandf1972.31.1.

[4] Gautam D, Forte G, Rodrigues H. Site effects and associated structural damage analysis in Kathmandu Valley, Nepal. Earthquakes Struct 2016;10:1013–32. doi:10.12989/eas.2016.10.5.1013.

[5] Jeong S, Bradley BA. Amplification of strong ground motions at Heathcote Valley during the 2010–2011 Canterbury earthquakes: Observation and 1D site response analysis. Soil Dyn Earthq Eng 2017;100:345–56. doi:10.1016/J.SOILDYN.2017.06.004.

[6] Sextos A, De Risi R, Pagliaroli A, Foti S, Passeri F, Ausilio E, et al. Local site effects and incremental damage of buildings during the 2016 Central Italy earthquake sequence. Earthq Spectra 2018:100317EQS194M. doi:10.1193/100317EQS194M.

[7] Bradley BA. A framework for validation of seismic response analyses using seismometer array recordings. Soil Dyn Earthq Eng 2011;31:512–20. doi:10.1016/J.SOILDYN.2010.11.008.

[8] Elgamal A-W, Zeghal M, Parra E, Gunturi R, Tang HT, Stepp JC. Identification and modeling of earthquake ground response — I. Site amplification. Soil Dyn Earthq Eng 1996;15:499–522. doi:10.1016/S0267-7261(96)00021-8.

[9] Borcherdt RD, Glassmoyer G. On the characteristics of local geology and their influence on ground motions generated by the Loma Prieta earthquake in the San Francisco Bay region, California. Bull Seismol Soc Am 1992;82:603–41.

[10] Borcherdt RD. Estimates of Site-Dependent Response Spectra for Design (Methodology and

Justification). Earthq Spectra 1994;10:617–53. doi:10.1193/1.1585791.

[11] Comina C, Foti S, Boiero D, Socco L V. Reliability of VS,30 evaluation from surface-wave tests. J Geotech Geoenvironmental Eng 2011;137:579–86. doi:10.1061/(ASCE)GT.1943-5606.0000452.

[12] Ohta Y, Goto N. Empirical shear-wave velocity equations in terms of characteristic soil indexes. Earthq Eng Struct Dyn 1978;6:167–87. doi:10.1002/eqe.4290060205.

[13] Pitilakis K, Raptakis D, Lontzetidis K, Tika-Vassilikou T, Jongmans D. Geotechnical and geophysical description of euro-seistests, using field and laboratory tests and moderate strong ground motions. J Earthq Eng 1999;3:381–409. doi:10.1080/13632469909350352.

[14] Fabbrocino S, Lanzano G, Forte G, Santucci de Magistris F, Fabbrocino G. SPT blow count vs. shear-wave velocity relationship in the structurally complex formations of the Molise Region (Italy). Eng Geol 2015;187:84–97. doi:10.1016/J.ENGGEO.2014.12.016.

[15] Boore DM, Stewart JP, Seyhan E, Atkinson GM. NGA-West2 equations for predicting PGA, PGV, and 5% damped PSA for shallow crustal earthquakes. Earthq Spectra 2014;30:1057–85. doi:10.1193/070113EQS184M.

[16] Campbell KW, Bozorgnia Y. NGA-West2 ground motion model for the average horizontal components of PGA, PGV, and 5% damped linear acceleration response spectra. Earthq Spectra 2014;30:1087–115. doi:10.1193/062913EQS175M.

[17] Akkar S, Sandıkkaya MA, Bommer JJ. Empirical ground-motion models for point- and extended-source crustal earthquake scenarios in Europe and the Middle East. Bull Earthq Eng 2014;12:359–87. doi:10.1007/s10518-013-9461-4.

[18] Lanzano G, Luzi L, Pacor F, Felicetta C, Puglia R, Sgobba S, et al. A revised ground-motion prediction model for shallow crustal earthquakes in Italy n.d. doi:10.1785/0120180210.

[19] Akkar S, Bommer JJ. Empirical equations for the prediction of PGA, PGV, and spectral accelerations in Europe, the Mediterranean Region, and the Middle East. Seismol Res Lett 2010;81:195–206. doi:10.1785/gssrl.81.2.195.

[20] Bindi D, Pacor F, Luzi L, Puglia R, Massa M, Ameri G, et al. Ground motion prediction equations derived from the Italian strong motion database. Bull Earthq Eng 2011;9:1899–920. doi:10.1007/s10518-011-9313-z.

[21] Bindi D, Massa M, Luzi L, Ameri G, Pacor F, Puglia R, et al. Pan-European ground-motion prediction equations for the average horizontal component of PGA, PGV, and 5 %-damped PSA at spectral periods up to 3.0 s using the RESORCE dataset. Bull Earthq Eng 2014;12:391–430. doi:10.1007/s10518-013-9525-5.

[22] Cauzzi C, Faccioli E. Broadband (0.05 to 20 s) prediction of displacement response spectra based on worldwide digital records. J Seismol 2008;12:453–75. doi:10.1007/s10950-008-9098-y.

[23] BSSC. NEHRP Recommended provisions for seismic regulations for new buildings and other structures 1998.

[24] CEN. European Committee for Standardization. Eurocode 8: design provisions for earthquake resistance of structures 2003.

[25] Steidl JH. Site response in Southern California for probabilistic seismic hazard analysis. Bull Seismol Soc Am 2000;90:S149–69. doi:10.1785/0120000504.

[26] Choi Y, Stewart JP. Nonlinear site amplification as function of 30 m shear-wave velocity. Earthq Spectra 2005;21:1–30. doi:10.1193/1.1856535.

[27] Lee VW, Trifunac MD. Should average shear-wave velocity in the top 30 m of soil be used to describe seismic amplification? Soil Dyn Earthq Eng 2010;30:1250–8. doi:10.1016/J.SOILDYN.2010.05.007.

[28] Anbazhagan P, Sheikh MN, Parihar A. Influence of rock depth on seismic site classification for shallow bedrock regions. Nat Hazards Rev 2013;14:108–21. doi:10.1061/(ASCE)NH.1527-6996.0000088.

[29] Bouckovalas G, Papadimitriou A, Karamitros D. Compatibility of EC-8 ground types and site effects with 1-D wave propagation theory. Work. ETC12 Eval. Comm. Appl. EC8, 1992.

[30] Pitilakis K, Riga E, Anastasiadis A. New code site classification, amplification factors and normalized response spectra based on a worldwide ground-motion database. Bull Earthq Eng 2013;11:925–66. doi:10.1007/s10518-013-9429-4.

[31] CS.LL.PP. Decreto Ministeriale: Norme tecniche per le costruzioni, Gazzetta Ufficiale della Repubblica Italiana, n. 42, 20 febbraio, Suppl. Ordinario n. 8. Ist. Polig. e Zecca dello Stato S.p.a., Rome (in Italian). 2018.

[32] ISSMGE. Manual for zonation on seismic geotechnical hazards (revised version). 1993.

[33] Ansal A, Kurtuluş A, Tönük G. Seismic microzonation and earthquake damage scenarios for urban areas. Soil Dyn Earthq Eng 2010;30:1319–28. doi:10.1016/J.SOILDYN.2010.06.004.

[34] Wills CJ, Clahan KB. Developing a map of geologically defined site-condition categories for california. Bull Seismol Soc Am 2006;96:1483–501. doi:10.1785/0120050179.

[35] Chiou B, Darragh R, Gregor N, Silva W. NGA project strong-motion database. Earthq Spectra 2008;24:23–44. doi:10.1193/1.2894831.

[36] Lee C-T, Tsai B-R. Mapping Vs30 in Taiwan. Terr Atmos Ocean Sci 2008;19:671. doi:10.3319/TAO.2008.19.6.671(PT).

[37] Cantore L, Convertito V, Zollo A. Development of a site-conditions map for the Campania-Lucania region (southern Apennines, Italy). Ann Geophys 2010;53:27–37. doi:10.4401/ag-4648.

[38] Yong A. Comparison of measured and proxy-based V S 30 values in California. Earthq Spectra 2016;32:171–92. doi:10.1193/013114EQS025M.

[39] Parker GA, Harmon JA, Stewart JP, Hashash YMA, Kottke AR, Rathje EM, et al. Proxy-Based V_{S30} Estimation in Central and Eastern North America. Bull Seismol Soc Am 2017;107:117–31. doi:10.1785/0120160101.

[40] Thompson EM, Wald DJ, Worden CB. A VS30 map for California with geologic and topographic constraints. Bull Seismol Soc Am 2014;104:2313–21. doi:10.1785/0120130312.

[41] Allen TI, Wald DJ. Topographic slope as a proxy for seismic site-conditions (VS30) and

682 amplification around the globe. 2007. doi:10.3133/OFR20071357.
683 [42] Lemoine A, Douglas J, Cotton F. Testing the applicability of correlations between
684 topographic slope and VS30 for Europe. Bull Seismol Soc Am 2012;102:2585–99.
685 doi:10.1785/0120110240.
686 [43] Forte G, Fabbrocino S, Fabbrocino G, Lanzano G, Santucci de Magistris F, Silvestri F. A
687 geolithological approach to seismic site classification: an application to the Molise Region
688 (Italy). Bull Earthq Eng 2017;15:175–98. doi:10.1007/s10518-016-9960-1.
689 [44] Luzi L, Meroni F. Deliverable 6: Valutazioni sperimentali di amax e di spettri di risposta
690 calibrate per le condizioni locali (in italian). 2007.
691 [45] Michelini A, Faenza L, Lauciani V, Malagnini L. Shakemap implementation in Italy.
692 Seismol Res Lett 2008;79:688–97. doi:10.1785/gssrl.79.5.688.
693 [46] Di Capua G, Peppoloni S, Amanti M, Cipolloni C, Conte G. Site classification map of Italy
694 based on surface geology. Geol Soc London, Eng Geol Spec Publ 2016;27:147–58.
695 doi:10.1144/EGSP27.13.
696 [47] Wald DJ, Quitoriano V, Heaton TH, Kanamori H, Scrivner CW, Worden CB. TriNet
697 “ShakeMaps”: rapid generation of peak ground motion and intensity maps for earthquakes in
698 Southern California. Earthq Spectra 1999;15:537–55. doi:10.1193/1.1586057.
699 [48] Pal JD, Atkinson GM. Scenario shakemaps for Ottawa, Canada. Bull Seismol Soc Am
700 2012;102:650–60. doi:10.1785/0120100302.
701 [49] CS.LL.PP. Decreto Ministeriale 14 gennaio 2008: Norme tecniche per le costruzioni,
702 Gazzetta Ufficiale della Repubblica Italiana, n. 29, 4 febbraio, Suppl. Ordinario n. 30. Ist.
703 Polig. e Zecca dello Stato S.p.a., Rome (in Italian). 2008.
704 [50] Boore DM. Estimating Vs (30) (or NEHRP site classes) from shallow velocity models
705 (depths < 30 m). vol. 94. 2004.
706 [51] Boore DM, Thompson EM, Cadet H. Regional correlations of VS30 and velocities averaged
707 over depths less than and greater than 30 meters. Bull Seismol Soc Am 2011;101:3046–59.

708 doi:10.1785/0120110071.
709 [52] Kuo C-H, Wen K-L, Hsieh H-H, Chang T-M, Lin C-M, Chen C-T. Evaluating empirical
710 regression equations for Vs and estimating Vs30 in northeastern Taiwan. Soil Dyn Earthq
711 Eng 2011;31:431–9. doi:10.1016/J.SOILDYN.2010.09.012.
712 [53] ASTM. D7400-08 Standard test methods for downhole seismic testing. Annu B ASTM Stand
713 Am Soc Test Mater 2008.
714 [54] Stucchi M, Meletti C, Montaldo V, Crowley H, Calvi GM, Boschi E. Seismic hazard
715 assessment (2003-2009) for the Italian building code. Bull Seismol Soc Am 2011;101:1885–
716 911. doi:10.1785/0120100130.
717 [55] Amanti M, Bontempo R, Cara P, Conte G, Di Bucci D, Lembo P, et al. Interactive geological
718 map of Italy, 1:100.000. SGN, SSN, ANAS 3 CD-Rom 2002.
719 [56] Stewart JP, Klimis N, Savvaidis A, Theodoulidis N, Zargli E, Athanasopoulos G, et al.
720 Compilation of a local VS profile database and its application for inference of VS30 from
721 geologic- and terrain-based proxies. Bull Seismol Soc Am 2014;104:2827–41.
722 doi:10.1785/0120130331.
723 [57] Peccerillo A. Plio-Quaternary volcanism in Italy : petrology, geochemistry, geodynamics.
724 Springer; 2005.
725 [58] McGill R, Tukey JW, Larsen WA. Variations of Box Plots. Am Stat 1978;32:12.
726 doi:10.2307/2683468.
727 [59] Horton RE. Erosional development of streams and their and their drainage basins;
728 hydrophysical approach to quantitative morphology. GSA Bull 1945;56:275–370.
729 doi:10.1130/0016-7606(1945)56[275:edosat]2.0.co;2.
730 [60] Cornell CA. Engineering seismic risk analysis. Bull Seismol Soc Am 1968;58:1583–606.
731 doi:http://dx.doi.org/10.1016/0167-6105(83)90143-5.
732 [61] Ambraseys NN, Simpson KA, Bommer JJ. Prediction of horizontal response spectra in
733 Europe. Earthq Eng Struct Dyn 1996;25:371–400. doi:10.1002/(SICI)1096-

9845(199604)25:4<371::AID-EQE550>3.0.CO;2-A.

[62] Meletti C, Galadini F, Valensise G, Stucchi M, Basili R, Barba S, et al. A seismic source zone model for the seismic hazard assessment of the Italian territory. Tectonophysics 2008;450:85–108. doi:10.1016/j.tecto.2008.01.003.

[63] Iervolino I, Chioccarelli E, Giorgio M. Aftershocks' effect on structural design actions in Italy. Bull Seismol Soc Am 2018;108:2209–20. doi:10.1785/0120170339.

[64] Chioccarelli E, Cito P, Iervolino I, Giorgio M. REASSESS V2.0: software for single- and multi-site probabilistic seismic hazard analysis. Bull Earthq Eng 2018:1–25. doi:10.1007/s10518-018-00531-x.